Cyclic AMP signalling and glucose metabolism mediate pH taxis by African trypanosomes

Sebastian Shaw[1,2,3], Sebastian Knüsel[1], Daniel Abbühl[1,4], Arunasalam Naguleswaran[1] and Isabel Roditi[1,*]

[1] Institute of Cell Biology, University of Bern, Bern, Switzerland

[2] Graduate School of Cellular and Biomedical Sciences, University of Bern, Bern, Switzerland

[3] Present address: Department of Pathobiology, School of Veterinary Medicine, University of Pennsylvania, 380 South University Avenue, Philadelphia, PA 19104, USA

[4] Present address: Trypanosome Cell Biology Unit, INSERM U1201, Institute Pasteur, 25 Rue du Docteur Roux, 75015 Paris, France

* Corresponding author: isabel.roditi@izb.unibe.ch

Abstract

More than a decade ago it was proposed that the collective migration of African trypanosomes on semi-solid surfaces could be explained by a combination of migration factors and repellents released by the parasites, but the identity of these molecules was unknown. Here we show that procyclic (insect midgut) forms acidify their environment as a consequence of glucose metabolism, generating pH gradients by diffusion. Early and late procyclic forms exhibit self-organising properties on surfaces. Both forms are attracted to alkali, but while early procyclic forms are repelled by acid and migrate outwards, late procyclic forms remain at the inoculation site. pH taxis relies on cyclic AMP signalling. Acid sensing requires a flagellar adenylate cyclase, ACP5, and a cyclic AMP response protein, CARP3, that interacts with ACP5. Deletion of the flagellar phosphodiesterase PDEB1 abolishes pH taxis completely. Trypanosomes can also respond to exogenously formed gradients. pH sensing is likely to be biologically relevant as trypanosomes experience large differences in pH as they progress through their tsetse fly host. In addition, self-generated gradients may help reinforce directionality. Moreover, since trypanosomes encode a large family of adenylate cyclases, these may govern other chemotactic responses and tissue tropisms in both the mammal and the fly.

Introduction

Environmental sensing, chemotaxis and quorum sensing present possibilities for pathogens to orient themselves within their hosts. All three are widespread in bacteria, and the sensors and response mechanisms have been characterised in detail [1,2]. Genes involved in bacterial chemotaxis and quorum sensing have long been linked to biofilm formation and swarming behaviour[3,4]. By contrast, very little is known about chemotaxis in unicellular eukaryotes, with the exception of *Dictyostelium discoideum*, which generates and reacts to cyclic AMP (cAMP) gradients, promoting aggregation and differentiation[5–8].

Intracellular pathogens frequently exploit receptor-ligand interactions to recognise and invade the appropriate cell types [9–12]. For extracellular parasites such as *Trypanosoma brucei spp*., causative agents of human and animal trypanosomiasis, it is not known what drives them to move from one host tissue to another. In their mammalian hosts, quorum sensing regulates the titre of *T. brucei* by triggering the differentiation of proliferative slender forms to quiescent stumpy forms[13,14]. When these are taken up by tsetse flies during a blood meal[15] they differentiate to early procyclic (midgut) forms and then to late procyclic forms[16]. In addition to the surface marker GPEET procyclin, which is only expressed by early procyclic forms, several metabolic enzymes, nutrient transporters and signal transducers are differentially expressed between the two forms[17,18]. Colonisation of the midgut by procyclic forms is followed by additional rounds of differentiation as parasites invade the proventriculus, then move to the salivary glands before being transmitted to a new mammalian host.

Early procyclic forms engage in a form of group migration, known as social motility (SoMo), when cultured on semi-solid surfaces such as agarose plates[18,19]. The parasites initially remain at the inoculation site, dividing approximately once every 24 h, then the communities start to form regularly spaced projections that extend by ~1 cm (500 body lengths) per day. Communities on the same plate are able to sense each other and reorient to avoid contact (Supplementary Video 1). Late procyclic forms do not exhibit SoMo, but they do produce a repellent that is sensed by early procyclic forms[18]. Communities on plates also react to other signals. Trypanosomes depleted of the spliced leader core protein SmD1 shed exosomes that act as repellents[20], while bacterial colonies can act as attractants[21]. Various species of *Leishmania*,

59 parasites related to trypanosomes, respond chemotactically to a range of compounds including
60 amino acids, carbohydrates and sera, in liquid culture[22–24]. In none of these cases is it known
61 which genes mediate the responses.

62 Few genes have been implicated in SoMo. Concomitant depletion of adenylate cyclases
63 ACP1&2, or depletion of ACP6 on its own, resulted in a hyper-social phenotype (hyper-SoMo)
64 where the communities formed more projections and migrated more rapidly, suggesting that
65 these are negative regulators[25]. The flagellar phosphodiesterase B1 (PDEB1)[19] and the
66 endoplasmic reticulum protein Rft1[26,27] are positive regulators of SoMo. Importantly, null
67 mutants of PDEB1 and Rft1 were not only impaired in SoMo, but also defective in colonising the
68 tsetse midgut[26,28]. We postulated that SoMo is largely a chemotactic response to factors
69 produced by the trypanosomes themselves. Here we show that procyclic forms can generate pH
70 gradients through glucose metabolism and that the response of early and late procyclic forms to
71 these gradients can explain the self-organising properties of communities on plates. In addition,
72 we identified two cAMP signalling components involved in the response to acid, ACP5 and the
73 cAMP response protein CARP3. Notably, pH sensing is completely abolished in PDEB1-KO, where
74 cAMP levels are perturbed. pH taxis could be biologically relevant as there is a pH gradient in the
75 tissues that are colonised by the parasites during their transmission through the insect host [29].

76 **Results**

77 **Parasite-secreted factors change properties of the medium and repel migrating projections**

78 What are the factors causing collective migration in SoMo? The fact that communities sense and
79 avoid each other over considerable distances means that they react to attractants or repellents
80 that are secreted, or otherwise released, by the parasites. We started by investigating if these
81 factors were produced under normal growth conditions in liquid culture. We concentrated the
82 supernatant of a dense culture (2×10^7 cells ml^{-1}) 10-fold and spotted this "conditioned medium"
83 (CM) next to migrating projections on SoMo plates (Fig. 1a, upper panel). Projections migrating
84 towards the site where CM was spotted reoriented away from it, indicating that it was perceived
85 as a repellent. In a second experiment, CM was either sterile filtered or dialysed (with a 12 kDa
86 cut-off) prior to concentration and spotted next to migrating projections. As seen with untreated
87 CM, filtered CM still repelled migrating projections (Fig. 1a, lower left panel), but dialysed CM

88 lost its repellent properties (Fig. 1a, lower right panel). On the contrary, migrating parasites were
89 attracted to dialysed CM in the same way that they were to concentrated fresh medium (DTM)
90 (Fig. 1a). These results suggested that repellents might be metabolites that were lost upon
91 dialysis.

92 **Trypanosomes acidify their environment in liquid culture and on agarose plates**

93 Trypanosomes secrete a variety of molecules that influence the pH of their environment[30,31].
94 Indicators for pH, such as phenol red, are commonly used for culture media and it is apparent
95 that dense cultures are more acidic than fresh medium or log phase cultures, as illustrated for
96 early procyclic forms growing in liquid culture (Fig. 1b). We therefore used a small tip micro glass
97 pH electrode to measure the pH in liquid culture and on agarose plates (Fig. 2). Fresh medium
98 has a pH of 7.46 ($\pm$ 0.02) and the supernatant of a log phase culture has a pH of 7.45 ($\pm$ 0.01) (Fig.
99 2a). The pH decreased to 6.95 ($\pm$ 0.00) when parasites were allowed to overgrow; this
100 corresponds to ~3-fold increase in the concentration of H^+ ions (Fig. 2a).

101 To measure the pH on plates, 2 x 10^5 parasites were inoculated either in the centre of a
102 plate (Fig. 2b, left row), or in pairs at a defined distance from each other (Fig. 2b, right row), and
103 the pH was measured after 2, 3 ,4 and 7 days post inoculation. We measured the pH in the centre
104 of a community, at the periphery of a plate and between two communities. The pH at the centres
105 of the communities decreased from 7.50 to 7.31 ($\pm$ 0.05) during the first three days and
106 decreased further to 6.96 ($\pm$ 0.05) between days 3 and 7 (Fig. 2b, c). The pH at the periphery also
107 started to decrease between day 3 and 7, possibly because of diffusion of H^+ ions from the
108 parasite communities. When communities were plated in pairs, the pH at the midpoint between
109 them also decreased over time (Fig. 2b, right row, arrow). Thus, communities are able to acidify
110 their vicinity resulting in pH gradients on the plates.

111 We showed previously that trypanosomes needed to reach a threshold number before
112 they started migrating[18]. We now postulate that it is not the cell number that is critical, but rather
113 the need to establish a discernible pH gradient. When the same number of parasites were
114 inoculated onto plates containing different volumes of semi-solid medium, the time point at
115 which projections started to form was inversely proportional to the volume (Fig. 2d). This would

116 be consistent with larger volumes buffering the pH more effectively and requiring more cells, and
117 thus more time, before a gradient was established.

118 **Reaction of early and late procyclic forms to exposure to acid and alkali**

119 As a next step, we tested if manipulating the pH gradient had an influence on migration by
120 exposing early procyclic forms to external sources of acid or alkali (Fig. 3a, b). Early procyclic
121 forms were inoculated onto plates and incubated until the projections reached a length of about
122 2 cm. At this point, solutions of HCl or NaOH were pipetted onto the surface at a defined distance
123 (Fig. 3a) and the plates were incubated for 16-20 h. The migrating cells responded very strongly
124 to both solutions (Fig. 3b, Supplementary Videos 2 & 3). Exogenous NaOH acted as an attractant,
125 causing projections to reorient towards it (OH^- treatment), while HCl caused the projections to
126 stop moving outwards, or to move away from the acid (H^+ treatment). Using the same assay,
127 another 22 chemicals were tested (Supplementary Fig. 1). In most cases, when a solution was
128 acidic, the projections were repelled, and when a solution was basic, the cells were attracted to
129 it. These experiments also showed that the projections reacted to the pH rather than to specific
130 ions in the solutions.

131 We next tested late procyclic forms since these do not perform SoMo. Late procyclic
132 forms did not respond to HCl (Fig. 3c, Supplementary Video 4), but they formed a limited number
133 of projections that migrated towards NaOH. Community lifts (Fig. 3c) confirmed that the
134 parasites were still GPEET-negative and had not dedifferentiated to early forms. In summary,
135 these results demonstrate that procyclic forms exhibit pH taxis, with alkali acting as an attractant
136 for both early and late procyclic forms. In contrast, there are stage-specific differences in their
137 reaction to acid.

138 **RNA-seq analyses suggest that SoMo is a response to self-generated gradients**

139 To better understand the mechanisms behind self-organisation of early and late procyclic forms,
140 and their pH reponses, we performed RNA-seq under different conditions. A culture of procyclic
141 forms (>60 % GPEET-positive) was plated and allowed to form projections (Fig. 4a, far right). A
142 community lift with antibodies against procyclins showed that the tips were strongly positive for
143 GPEET, while the centre of the community stained more strongly for EP. Cells were isolated from

144 the tips and roots of projections (Fig. 4a far right) and analysed by RNA-Seq. Data confirmed that
145 markers of early procyclic forms were more highly expressed in the tips than the roots (Fig. 4a
146 left; Supplementary Table 1a). Other transcripts that were more highly expressed in the tip were
147 not characteristic of early procyclic forms in liquid culture, such as cysteine-rich acidic integral
148 membrane protein (CRAM)[32], a microtubule-associated repetitive protein (MARP2)[33] and a
149 hypothetical protein (hypo; Tb927.9.10400). In addition, several adenylate cyclases were
150 differentially expressed on plates; ACP3 and ACP5 were ≥2-fold higher in the tip, while ACP6 and
151 another adenylate cyclase (GRESAG 4; Tb927.11.1480) were ≥2-fold higher in the root. The up-
152 regulation of high affinity glucose transporters (THT2 and 2A), glycolytic enzymes and
153 components of the glycosome (Fig. 4a middle and Supplementary Table 1a) is suggestive of
154 higher glucose metabolism by the tip than the root. Increased expression of these transcripts is
155 also characteristic of early procyclic forms in liquid culture[17,18].

156 RNA-seq was also performed on the tips of communities exposed to acid or alkali (Fig. 4b
157 and Supplementary Table 1b). There were no significant differences (≥2-fold, p=0.05) between
158 non-exposed communities and those exposed to alkali. A single cation transporter (CatT,
159 Tb927.11.9000) was more highly expressed in cells exposed to acid, but the read counts were
160 extremely low in both cases. CatT and a copy of a contig (Tb11.v5.0514) were the only significant
161 differences in a comparison of acid- versus alkali-treated communities. Taken together, these
162 results suggest that self-generated pH gradients might be the normal driver of migration on SoMo
163 plates.

164 **Glucose contributes to the formation of pH gradients**

165 Since the RNA-seq data indicated that cells at the tip might metabolise glucose more actively
166 than cells at the root, we investigated the role of glucose in SoMo. For these experiments SDM80
167 medium was prepared with 1 mM glucose, 6 mM glucose or 6mM N-acetylglucosamine (GlcNAc),
168 which inhibits glucose uptake by binding to hexose transporters[34]. Early procyclic forms of Lister
169 427 Bern were inoculated onto plates and incubated for 6 days (Fig. 5a). The parasites in SDM80
170 with 1 mM glucose started migrating later than cells in SDM80 containing 6 mM glucose, and the
171 SoMo defect was even more pronounced when glucose uptake was blocked by GlcNAc. Under

172 these conditions the cells only formed rudimentary "knobs" at the edge of the community and
173 failed to form projections, even at later time points.

174 The reduced ability to migrate on plates can have a variety of causes, especially in the
175 context of glucose restriction. It might be due to longer population doubling times, motility
176 defects or inefficient energy metabolism. Procyclic cultures of Lister 427 Bern are stably GPEET-
177 positive[26,35]. Nevertheless, we assessed the proportion of early procyclic forms by flow cytometry
178 (Fig. 5b). Regardless of the medium in which the cells were grown, all cultures were ≥97% GPEET-
179 positive. Furthermore, the glucose concentration had no impact on the population doubling time
180 (Fig. 5c) or intracellular ATP levels (Fig. 5d), both assessed in liquid culture. Previous work showed
181 that directional motility is important for SoMo and migration through the fly[28]. We therefore
182 assessed cell motility (Fig. 5e); no differences were observed between cells grown in the presence
183 or absence of glucose.

184 To investigate whether different glucose concentrations influence the culture pH, we
185 compared medium alone with liquid cultures of trypanosomes in log phase or high density (Fig.
186 5f). While the pH of log-phase cultures did not differ from that of medium alone, dense cultures
187 of parasites in SDM79 or SDM80 with 6 mM glucose strongly acidified the medium. The
188 concentration of H^+ in dense cultures, compared to log phase cultures, increased 2.53-fold
189 (±0.03) for SDM79 and 2.51-fold (±0.06) for SDM80 plus glucose. By contrast, cells grown in
190 SDM80 plus GlcNAc showed a smaller change in H^+ ion concentration (1.22-fold ±0.03). We next
191 measured pH changes for communities growing on plates (Fig. 5g). The ΔpH between the centre
192 and the periphery reached -0.31(± 0.02) for parasites on SDM79 and -0.37(± 0.02) for SDM80 +
193 6mM glucose, corresponding to a ≥2-fold difference in H^+ ions at the two locations, whereas
194 plates containing SDM80 + GlcNAc did not show a difference in pH. Taken together, these data
195 show that glucose is required for parasites to generate a pH gradient, and that this correlates
196 with their ability to perform SoMo.

197 **Cyclic AMP signalling is involved in the response to pH**

198 RNA-seq identified a number of differentially expressed transcripts, including that of the flagellar
199 pocket protein CRAM, which was more highly expressed in the tips than in the roots (Fig. 4a).
200 CRAM is not essential in procyclic culture forms[36]. When we generated knockouts, these grew at

201 the same rate as their parental line, but two out of three independent clones produced smaller
202 projections. Nevertheless, all three reacted to acid and alkali in the same way as wild-type cells
203 (Supplementary Fig. 2) so we did not proceed with additional analyses.
204 Several adenylate cyclases were also differentially expressed between the tip and the root
205 (Fig. 4a). Before we started analysing these and other members of the cAMP signalling pathway,
206 we tested whether PDEB1, which hydrolyses cAMP, had an influence on the pH response. When
207 the PDEB1 null mutant was exposed to alkali or acid, it showed no pH response (Fig. 6a). Notably,
208 the PDEB1 null mutant differs from both early procyclic forms, which react to acid and alkali, and
209 late procyclic forms, which form projections in response to alkali but do not respond to acid.
210 Four cAMP response proteins (CARP1-CARP4) were previously identified in an RNAi
211 screen as mediating resistance to an inhibitor of PDEB1[37], but they have not been studied in the
212 context of SoMo. For CARP 1 and 2, we only obtained clones after single rounds of transfection.
213 We did not pursue these further, however, as the resistance genes were not integrated at the
214 correct loci. However, we were able to obtain knockouts of CARP3 and 4 (Supplementary Fig. 3a).
215 CARP4 null mutants did not show any difference to the parental line when they were subjected
216 to a standard SoMo assay or tested for pH responses (data not shown). Deletion of CARP3, while
217 not affecting growth in liquid culture, motility or expression of the early marker GPEET
218 (Supplementary Fig. 3b-3e) resulted in a major SoMo defect, reminiscent of the PDEB1 null
219 mutant (Fig 6b, upper panel). CARP3 knockouts still reacted to alkali, but did not react to acid (Fig
220 6b, lower panel). An HA-tagged addback of CARP3, expressed from a procyclin locus, partially
221 rescued the SoMo phenotype (Fig 6b, upper panel), although the projections were shorter than
222 in the parental line. Importantly, the addback was now able to sense and react to both acid and
223 alkali (Fig 6b, lower panel).
224 CARP3 is distributed between the cytoplasm and the flagellum (Supplementary Fig. 3f;
225 www.tryptag.org). Since no interaction partners have been reported, a pulldown was performed
226 with HA-tagged CARP3 (Fig. 6e) and analysed by mass spectrometry. This led to the identification
227 of adenylate cyclases ACP3 and ACP5 in three biological replicates (Supplementary Table 2).
228 These interactions were confirmed by *in situ* tagging and co-immunoprecipitation of myc-tagged
229 versions of ACP3 and ACP5 in the CARP3-HA addback line (Fig. 6e). The reciprocal co-

230 immunoprecipitations with anti-myc antibody confirmed the interaction for both ACP3 and ACP5.
231 These results, combined with their differential expression in the tips and roots of projections (Fig.
232 4a) stimulated us to revisit some of the flagellar ACP previously characterised by Lopez and
233 coworkers[25]. In their study they showed that knockdown of ACP1/2 or ACP6 by RNAi resulted in
234 a hyper-SoMo phenotype. We obtained null mutants of ACP2 and ACP6, but it was only possible
235 to generate single knockouts of ACP1 and ACP5 (Supplementary Fig. 4a) implying that they are
236 essential at this stage of the life cycle. Although we attempted to knock out ACP3, and isolated
237 resistant cell lines, the antibiotic resistance genes were not integrated at the correct locus (data
238 not shown). The full knockout of ACP6 and the semi-knockout of ACP1 both exhibited hyper-
239 SoMo phenotypes, while the full knockout of ACP2 showed no phenotype (Supplementary Fig.
240 4b). These results are consistent with the findings with the RNAi lines; they also indicate that the
241 hyper-SoMo phenotype in the previously published ACP1/2 RNAi line[25] was due to depletion of
242 ACP1. Unexpectedly, however, and in contrast to the results with RNAi[25], single knockouts of
243 ACP5 were unable to form projections on plates (Fig. 6c, upper panel). In terms of their pH
244 response, ACP5 single knockouts resembled CARP3 double knockouts - they were able to form
245 projections migrating towards an alkaline source, but were refractory to acid (Fig. 6c, lower
246 panel). Further experiments showed that >80% of these cells were GPEET-positive and that the
247 phenotype of the ACP5 mutants was not due to defects in growth or motility (Supplementary Fig.
248 4c-4f). These experiments also revealed that ACP5-myc was localised exclusively at the flagellar
249 tip (Fig 6d). In summary, we have extended the catalogue of cAMP signalling components that
250 are involved in regulating SoMo. In addition, the finding that PDEB1, ACP5 and CARP3 play a role
251 in the perception of environmental acidity/alkalinity is consistent with SoMo being a response to
252 self-generated pH gradients.

253 **Discussion**

254 It was proposed more than a decade ago that the collective migration of trypanosomes on plates
255 could be explained by a combination of migration factors and repellents released by the
256 parasites[19], but the identity of these molecules was unknown. Here we show that trypanosomes
257 acidify their environment as a consequence of glucose metabolism, generating pH gradients by
258 diffusion. While it is commonly assumed that free glucose levels in tsetse are low between blood

259 meals, it is difficult to identify a primary publication on this topic. It was shown, however, that
260 the fly gut contains trehalose, a disaccharide composed of two glucose subunits[38]. Moreover, *T.*
261 *b. brucei* encodes a putative α-trehalose phosphorylase (Tb927.11.10670) which could generate
262 glucose and glucose-1-phosphate. Early and late procyclic forms exhibit self-organising
263 properties. It is the perception of these self-generated pH gradients that governs the outward
264 migration of early procyclic forms towards a more alkaline environment, while late procyclic
265 forms remain at the inoculation site. Local acidification of the environment, and the perception
266 thereof, can also explain the spacing between projections emanating from the same parasite
267 colony, as well as the cessation of migration or the reorientation of projections from two separate
268 communities on the same plate. In addition, it explains why the start of migration is not solely
269 dependent on a threshold cell number, as was previously reported[18], but rather on the external
270 pH. Early procyclic forms are also able to perceive exogenous sources of acid and alkali as
271 repellents and attractants, respectively. Late procyclic forms are also attracted to a more basic
272 environment, but unlike early procyclic forms they are not repelled by acid, explaining why they
273 remain at the inoculation site on plates and do not perform SoMo.

274 Analyses of the transcriptomes of cells spontaneously performing SoMo, or reacting to
275 exogenous alkali or acid, are consistent with them being the same response. Comparison of the
276 transcriptomes of trypanosomes at the tips and roots of projections showed that migrating cells
277 at the tip expressed high levels of markers for early procyclic forms. This mirrors what is seen in
278 liquid culture[17,18] as well as at early time points after flies are infected with stumpy forms (AN
279 and IR, manuscript in preparation). Among the adenylate cyclases differentially expressed
280 between the tip and the root, ACP6 is more highly expressed at the root and is also up-regulated
281 in late procyclic forms. By contrast, ACP3 and ACP5, which are more highly expressed in the tip,
282 are not stage-regulated between early and late procyclic forms in liquid culture[17]. This is also true
283 of a few other transcripts, such as CRAM, and may reflect a response to culture on plates.

284 cAMP signalling is required for the perception of pH gradients (summarised in Fig 6f). A
285 PDEB1 knockout was not only defective in SoMo[28], but was also impervious to acid and alkali. In
286 contrast to an RNAi mutant of ACP5 which still performed SoMo normally[25], an ACP5 single
287 knockout did not form projections and was insensitive to exogenous acid, but was still attracted

288 to alkali. In this respect, its behaviour resembles that of late procyclic forms. Down-regulation or
289 deletion of ACP6 ([25] and Supplementary Fig. 4b) or deletion of one copy of ACP1 cause hyper-
290 SoMo, while ACP2 is not required for SoMo or pH taxis. ACP1, ACP5 and ACP6 are localised at the
291 flagellar tip ([39] and Fig. 6d), highlighting its importance as a sensor.

292 For the first time, we show that there is a physical link between a cyclic AMP response
293 protein, CARP3, and adenylate cyclases ACP3 and ACP5. Moreover, the CARP3 null mutant had
294 the same defects in SoMo and acid sensing as the ACP5 single knockout. Interestingly, there is
295 strong evidence that CARP3 is N-myristoylated[40], which could enable it to associate with the inner
296 leaflet of the plasma membrane. N-myristoylation has been shown to regulate signalling in
297 mammals[41] and it is conceivable that acylated and non-acylated forms of CARP3 enable signals
298 to be transmitted from the membrane to the interior of the cell. *T. brucei*, which has the most
299 complex life cycle of all the African trypanosomes, also encodes the largest number of adenylate
300 cyclases. Many of these are stage-regulated, and it is plausible that they have functions in
301 reacting to their local environment.

302 pH taxis by trypanosomes is likely to be biologically relevant during fly transmission as
303 there are large differences between the pH of the midgut (pH ~8) and proventriculus (pH ~10.5)[29].
304 This would enable parasites to follow cues provided by the fly as they migrate to different
305 compartments. It is established that procyclic forms respond chemotactically to other effectors
306 [20,21], but their identities are unknown. Chemotaxis may also explain how parasites in the
307 mammalian host disperse from the bloodstream into other tissues [42–44]. Finally, the concept that
308 self-generated gradients help drive directionality and speed expansion into new territories,
309 recently described for bacteria[45], may also apply to trypanosomes.

310 **Methods**

311 **Trypanosome stocks and culture conditions**

312 Procyclic forms of EATRO1125 were derived from bloodstream forms of *T. b. brucei* AnTat1.1[46].
313 Early procyclic forms were cultivated at 27 °C and 2.5 % CO_2 in DTM supplemented with 15 %
314 foetal bovine serum (FBS) [47]. Late procyclic forms were cultured in SDM79[48] containing 10 % FBS
315 at 27 °C. Parasites were maintained at a density between 10^6 and 10^7 cells ml^{-1}. Procyclic forms
316 of *T. b. brucei* Lister 427 and derivatives thereof were cultured in SDM79 or SDM80 containing

317 10 % FBS at 27 °C. SDM80 components were as described[49], except that BME vitamin solution
318 100x (Bioconcept 5-20K00-H) was used instead of vitamin mix 100x (Invitrogen 010144) and 1%
319 Pen/Strep 10'000 IU/µg (Bioconcept 4-01F00-H) was used instead of 0.1 mM kanamycin. Glucose-
320 free SDM80 medium was supplemented with 10% FBS, which results in a final concentration of
321 ~1 mM glucose. If indicated, SDM80 + 10 % FBS was supplemented with 6 mM D-glucose or 6 mM
322 N-Acetyl-D-glucosamine (GlcNAc) from a 1.2 M stock solution in water. Population doubling
323 times were determined over a period of at least 5 days in which the cell density was determined
324 daily.

325 **SoMo assays and community lifts**

326 The protocol to produce plates was adapted from Imhof and coworkers[18]. Plates were always
327 used on the same day that they were poured. Culture medium (10 ml) supplemented with 0.4 %
328 agarose (Promega V3125) was poured into petri dishes (85 mm diameter). Open plates were then
329 air-dried for 1 hour in a laminar flow hood. Cells from an exponentially growing culture were
330 centrifuged briefly and resuspended in the residual medium at a density of 4×10^7 cells ml^{-1}. Two
331 hundred thousand cells were spotted per inoculum; plates were sealed with parafilm and
332 incubated in a humidified environment at 27 °C and 2.5 % CO_2. Photographs of plates were taken
333 using a Nikon E8400 camera.

334 Community lifts for the detection of GPEET and EP procyclins were performed as
335 described[18], using nitrocellulose filters (Whatman Protran BA85), K1 rabbit anti-GPEET[35] at a
336 dilution of 1:1000 and TBRP1/247 mouse anti-EP (Cat. no. CLP001A, Cedarlane Laboratories,
337 Burlington, Canada) at a dilution of 1:2500 as primary antibodies (1 h incubation time at room
338 temperature). The secondary antibodies goat anti-mouse IRDye 800CW (LI-COR Biosciences, Bad
339 Homburg, Germany) and goat anti-rabbit IRDye 680LT (LI-COR Biosciences) were used at dilutions
340 of 1:10000 (1 h incubation time at room temperature). The filters were rinsed 3 times in TBS +
341 0.05 % Tween (Sigma), followed by one final rinse in PBS before being dried overnight at room
342 temperature and scanned on a LI-COR Odyssey Infrared Imager model 9120, using Odyssey
343 Application Software, Version 3.0.21.

344 **pH measurements on SoMo plates and in liquid cultures**

345 To monitor pH changes in liquid culture and on agarose plates, trypanosomes were cultured in a
346 humidified incubator at 27 °C and 2.5 % CO_2. SoMo plates were kept in the same incubator,
347 without sealing the lids with parafilm. For analysis of growth rate and pH measurements, cells
348 were maintained between 1 – 10 x 10^6 cells ml^{-1} by daily monitoring and dilution. "Log-phase"
349 samples had densities of 3 – 9 x 10^6 cells ml^{-1}. If not stated otherwise, "dense" samples were
350 obtained from cultures with a concentration of 1 - 1.5 x 10^7 cells ml^{-1} without further dilution for
351 2 days. "Medium only" refers to complete medium incubated in a culture flask in a humidified
352 incubator at 27 °C and 2.5 % CO_2 for at least 12 h. The pH of culture supernatants or SoMo plates
353 was measured using a micro electrode (Thermo Scientific™ Orion™ 9810BN Micro pH Electrode;
354 fisher scientific).

355 **Preparation of concentrated supernatant**

356 Early procyclic forms were grown until they reached a concentration of 3 x 10^7 cells ml^{-1}. The cells
357 were centrifuged for 5 minutes at 2500 g and the conditioned medium was transferred to a new
358 tube. Conditioned medium was either concentrated directly or first sterile filtered (Jet Biofil
359 syringe filter, 0.22 µm, REF: FVP203030K) or dialysed. 2 ml of conditioned medium were dialysed
360 with dialysis tubing cellulose membranes (Sigma-Aldrich, cut-off 12 kDa, REF: D9777-100FT)
361 against 50 ml DTM supplemented with 15 % FBS at 4 °C in two rounds (16 hours, then 12 hours).
362 To concentrate the conditioned medium, 1 ml was transferred into a 1.5 ml Eppendorf tube and
363 vacuum centrifuged for several hours until 100 µl remained in the tube. As a control, DTM only
364 was concentrated in parallel.

365 **pH taxis assay**

366 Procyclic forms were inoculated onto plates as described for SoMo assays. Following incubation
367 at 27 °C for four days, concentrates of 30 µl conditioned medium or medium only, or different
368 chemical solutions were added to the plates at a distance of 1.5 cm from migrating projections
369 (Fig. 3a, D = distance). The plates were sealed with parafilm and incubated at 27 °C for 16-20
370 hours. Stock solutions were prepared at a concentration of 1M, if not stated otherwise.

371 **Hot phenol extraction of RNA from migrating tips**

372 Plates containing semi-solid DTM medium were inoculated with 2 x 10^5 cells from a culture of
373 procyclic form EATRO1125 (60 – 80 % GPEET-positive). Following incubation for 6 – 7 days, tip
374 and root samples were collected from projections that were ≥2.5 cm long. For collecting tips
375 reacting to acid or alkali, 3 x 10^5 cells were seeded, incubated for five days and then 30 µl 1M
376 NaOH or 1M HCl were added on two sides of migrating cells at a distance of 1.5 cm from the tips
377 (Fig. 3a, D = distance). In total, between 70-100 tips of migrating projections, that were exposed
378 to acidic or alkaline solutions for 16 hours, were harvested. Only tips that clearly showed a
379 reaction were collected (usually 5-7 tips per community).

380 Cells were harvested by punching out a piece of agarose using an inverted P2 micro tip
381 (outer and inner diameters 6 and 4.5 mm, respectively). The tip subpopulation refers to the
382 outermost 3 mm of protrusions. The root refers to the region at the base of the projection as
383 shown in Figure 4a. Between 20-25 tips or 3-5 root samples were transferred into 1 ml DTM in a
384 24-well plate well. Cells were washed off the agarose pieces by careful rinsing with a P1000
385 pipette and the cell suspension was transferred to a 1.5 ml Eppendorf tube. The agarose pieces
386 were rinsed once more with 0.5 ml DTM, added to the cell suspension and centrifuged for 2
387 minutes at 3300 x g. On average, approximately 1 x 10^5 cells were retrieved from each tip and 6
388 x 10^5 cells from each root sample. For tips reacting to acid or alkali, the wells of a 6-well plate
389 contained a larger number of samples (up to 100 tips). In this case, the supernatant was carefully
390 aspirated from the well and collected in a 15 ml Falcon tube and the agarose pieces were washed
391 twice with 4 ml medium. The washes were added to the cells in the 15 ml Falcon tube and
392 centrifuged for 5 minutes at 2500 g. Cell pellets were resuspended in 50 µl residual medium and
393 RNA was extracted with hot phenol as described[50].

394 **RNA-seq analysis**

395 Total RNA (maximum 10 µg) was processed and used for Illumina sequencing as described
396 previously[17]. Poly(A)-selected RNAs were used for the preparation of cDNA libraries using an
397 Illumina TruSeq kit. Sequencing of cDNA libraries was performed at Fasteris, Geneva, using
398 Illumina HiSeq sequencing systems with 150 bp read lengths and sequencing depths of
399 approximately 20 million reads per sample. Reads were mapped to the *T. b. brucei* 927 reference

400 genome version 5.1, using the bowtie tool available in the Galaxy Interface (usegalaxy.org) with
401 default parameters that allow a maximum of 2 mismatches per 28 bp seed (Galaxy version
402 1.1.2). Read counts were extracted using "Feature-count" tool available in Galaxy using
403 TritrypDB-41 GFF annotation file. DESeq2 analysis were performed to identify the differentially
404 regulated genes and RPM values were calculated to estimate the transcripts abundance. Raw
405 read files are deposited at the European Nucleotide Archives (ENA) http://www.ebi.ac.uk/ena as
406 study PRJEB41935.

407 **Flow cytometry**

408 Cells were fixed in 2 % (w/v) PFA/PBS at 4°C overnight at a concentration of 1 x 10^7 cells ml^{-1} and
409 processed for flow cytometric analysis as previously described[51,52]. Rabbit antiserum α-GPEET
410 K1[35] and Alexa Fluor 488-conjugated secondary antibody (Invitrogen, Thermo Fisher Scientific)
411 were used at 1:1000 dilution in 2 % BSA/PBS and incubated for 1.5 h at 4°C with rotation. To
412 remove particles of subcellular size, a cut-off of 7.5 x 10^5 was applied to the forward scatter. A
413 total of ten thousand events were recorded using a ACEA NovoCyte flow cytometer and analysed
414 without gating using FlowJo software version 10.6.1 (BD Life Sciences).

415 **Determination of steady-state ATP levels**

416 ATP concentrations were measured based on a previously described ATP production assay[53]. To
417 measure steady-state ATP levels in whole cells, cells were washed twice in ice-cold PBS and
418 resuspended in PBS at 2.5 x 10^7 cells ml^{-1}. Denaturation with perchloric acid, precipitation and
419 neutralisation with KOH was performed as described[53]. The cleared lysate was serially diluted 4-
420 fold in H_2O. Routinely, cells were harvested in triplicate and the second dilution of the cleared
421 lysate (16-fold dilution) was used for the bioluminescence assay. For each replicate, ATP
422 concentrations were measured in triplicate. ATP concentrations were determined using the ATP
423 Bioluminescence Assay Kit CLS II (Roche 11699695001, from Sigma-Aldrich) according to
424 manufacturer's instructions. For each dilution, 10 µl was added to 40 µl of 0.5 M Tris-acetate, pH
425 7.75 and supplemented with luciferase reagent to a final volume of 100 µl. Titrations of the ATP
426 standard supplied were analysed in parallel. Luminescence was measured in 96-well microtitre
427 plates (opaque, non-binding) using a Turner BioSystems Modulus Microplate Luminometer,

428 Model 9300-001. Signals were integrated over 5 sec in steady-glo mode. Three readings per plate
429 were acquired, with a period of 10 min. Values of the second reading were used for analysis,
430 since only the second and third readings yielded stable signals.

431 **Motility assays**

432 Cultures were allowed to grow to a density between 4 - 7 x 10^6 cells ml^{-1} and adjusted to a final
433 concentration of 5 x 10^6 prior to the experiment. These cells (in medium) were placed into
434 motility chambers[54]. To prevent cell adherence, the chamber was precoated with 1 % poly L-
435 glutamic acid (Fisher Scientific, P4886-25MG) for one hour and washed twice with 70 % EtOH.
436 The chambers were then washed twice with 100 µl medium and once with cell suspension before
437 loading 100 µl of cells at a concentration of 5 x 10^6 cells ml^{-1}. The edges of the coverslip were
438 sealed to avoid evaporation and capillary flow of liquid. Time lapse movies were recorded at 200
439 ms, with 250 cycles and 10 x magnification with a Leica DM 5500B microscope. The dataset was
440 analysed with a tracking macro provided by Richard Wheeler, University of Oxford[55]. Velocity,
441 speed and individual cell tracks were plotted using Fiji version 1.0 [56] and Prism Version 6.

442 **Immunoprecipitation and proteomic analysis**

443 Isolation of HA-tagged protein complexes was performed as previously described[57] using the
444 addback cell line expressing CARP3-HA, or derivatives expressing CARP3-HA and either ACP3-myc
445 or ACP5-myc. Myc-tagged proteins were immunoprecipitated with 5 µg monoclonal antibody
446 9E10 (Cat No: MA1-980) and Dynabeads™ Pan Mouse IgG (Cat No: 11041), both from
447 ThermoFisher Scientific (Invitrogen). Isolated protein complexes were subjected to Western blot
448 analysis, or protein bands were cut from Coomassie-stained polyacrylamide gels, subjected to
449 trypsin digestion and proteins were identified by LC-tandem mass spectometry[58] at the
450 Proteomics and Mass Spectrometry Core Facility of the University of Bern.

451 **Generation of knockouts and addbacks**

452 Single knockouts, double knockouts and tagged addbacks were generated in the parental 427
453 Cas9 cell line[28]. Targeting cassettes were amplified from pPOTv7-hygromycin and pPOTv7-G418[59]
454 plasmids. The primers used for PCR amplification of the targeting fragments, the sgRNA
455 templates and the primers used for genotyping PCRs can be found in Supplementary Table 3. The

456 knockouts were verified by PCR (Supplementary Table 3). Transfection was performed as
457 described previously[60] using TbBSF transfection buffer [61]. Stable transformants were selected
458 using 15 µg ml^{-1} Geneticin G418 sulphate and 25 µg ml^{-1} hygromycin.

459 **Immunofluorescence analysis (IFA) of HA- and or Myc-tagged cells**

460 Cells were harvested at a density of 2 – 5 x 10^6 cells and then washed once with PBS. They were
461 left to settle on a coverslip for 20 minutes and then fixed with 4 % PFA in PBS for 4 minutes. After
462 removing the supernatant, the cells were permeabilized with Triton-x 100 diluted to 0.2 % in PBS
463 for 5 minutes and the liquid was aspirated. The samples were blocked in PBS + 4 % BSA for 1 hour
464 at RT. The primary antibodies (monoclonal α-HA rat 3F10 and monoclonal α-myc mouse 9E10,
465 from Roche, distributed by Sigma Aldrich) were diluted 1:1000 and 1:500 respectively in PBS +
466 0.4 % BSA and the samples incubated for 1 hour at RT. The cells were then washed 3 times with
467 PBS and the supernatant aspirated after every washing step. They were then incubated with the
468 secondary antibodies AlexaFluor 488 conjugated donkey α-rat (Life Technologies) and AlexaFluor
469 488 conjugated goat α-mouse (Invitrogen/Thermo Fisher) both diluted 1:2000 in PBS + 0.4 % BSA
470 for 1 hour at RT. The samples were then washed 3 times as described previously and incubated
471 with Hoechst 33342 (20µg/ml) diluted 1:500 in PBS for 2 minutes. After three washing steps, the
472 slides were mounted on microscope slides
473 with Mowiol and imaged with a Leica DM 5500B microscope with a 100x objective. The
474 acquired images were processed with Fiji[56].

475 **References**

476 1. Aframian, N. & Eldar, A. A Bacterial Tower of Babel: Quorum-Sensing Signaling Diversity
477 and Its Evolution. *Annu. Rev. Microbiol.* **74**, 587–606 (2020).
478 2. Yang, W. & Briegel, A. Diversity of Bacterial Chemosensory Arrays. *Trends Microbiol.* **28**,
479 68–80 (2020).
480 3. Daniels, R., Vanderleyden, J. & Michiels, J. Quorum sensing and swarming migration in
481 bacteria. *FEMS Microbiol. Rev.* **28**, 261–289 (2004).
482 4. Burkart, M., Toguchi, A. & Harshey, R. M. The chemotaxis system, but not chemotaxis, is
483 essential for swarming motility in *Escherichia coli*. *Proc. Natl. Acad. Sci. U. S. A.* **95**, 2568–

484 2573 (1998).
485 5. Tyson, J. J. & Murray, J. D. Cyclic AMP waves during aggregation of *Dictyostelium*
486 amoebae. *Development* **106**, 421–426 (1989).
487 6. Tomchik, K. J. & Devreotes, P. N. Adenosine 3',5'-monophosphate waves in *Dictyostelium*
488 *discoideum*: a demonstration by isotope dilution--fluorography. *Science* **212**, 443–446
489 (1981).
490 7. Maeda, M. *et al.* Periodic signaling controlled by an oscillatory circuit that includes
491 protein kinases ERK2 and PKA. *Science* **304**, 875–878 (2004).
492 8. Wang, M., Aerts, R. J., Spek, W. & Schaap, P. Cell cycle phase in *Dictyostelium discoideum*
493 is correlated with the expression of cyclic AMP production, detection, and degradation.
494 Involvement of cyclic AMP signaling in cell sorting. *Dev. Biol.* **125**, 410–416 (1988).
495 9. Kahn, S. *et al. Trypanosoma cruzi* amastigote adhesion to macrophages is facilitated by
496 the mannose receptor. *J. Exp. Med.* **182**, 1243–1258 (1995).
497 10. Kanjee, U. *et al. Plasmodium vivax* strains use alternative pathways for invasion. *J. Infect.*
498 *Dis.* (2020) doi:10.1093/infdis/jiaa592.
499 11. Kedzierski, L. *et al.* A leucine-rich repeat motif of *Leishmania* parasite surface antigen 2
500 binds to macrophages through the complement receptor 3. *J. Immunol.* **172**, 4902–4906
501 (2004).
502 12. Xing, M. *et al.* A Sialic Acid-Binding Protein SABP1 of *Toxoplasma gondii* Mediates Host
503 Cell Attachment and Invasion. *J. Infect. Dis.* **222**, 126–135 (2020).
504 13. Reuner, B., Vassella, E., Yutzy, B. & Boshart, M. Cell density triggers slender to stumpy
505 differentiation of *Trypanosoma brucei* bloodstream forms in culture. *Mol. Biochem.*
506 *Parasitol.* **90**, 269–280 (1997).
507 14. Vassella, E., Reuner, B., Yutzy, B. & Boshart, M. Differentiation of African trypanosomes is
508 controlled by a density sensing mechanism which signals cell cycle arrest via the cAMP
509 pathway. *J. Cell Sci.* **110 (Pt 2**, 2661–2671 (1997).
510 15. Rico, E. *et al.* Bloodstream form pre-adaptation to the tsetse fly in *Trypanosoma brucei*.
511 *Front. Cell. Infect. Microbiol.* **3**, 78 (2013).
512 16. Vassella, E. *et al.* A major surface glycoprotein of *trypanosoma brucei* is expressed

513 transiently during development and can be regulated post-transcriptionally by glycerol or
514 hypoxia. *Genes Dev.* **14**, 615–626 (2000).
515 17. Naguleswaran, A., Doiron, N. & Roditi, I. RNA-Seq analysis validates the use of culture-
516 derived *Trypanosoma brucei* and provides new markers for mammalian and insect life-
517 cycle stages. *BMC Genomics* **19**, 227 (2018).
518 18. Imhof, S., Knüsel, S., Gunasekera, K., Vu, X. L. & Roditi, I. Social motility of African
519 trypanosomes is a property of a distinct life-cycle stage that occurs early in tsetse fly
520 transmission. *PLoS Pathog.* **10**, e1004493 (2014).
521 19. Oberholzer, M., Lopez, M. A., McLelland, B. T. & Hill, K. L. Social motility in african
522 trypanosomes. *PLoS Pathog.* **6**, e1000739 (2010).
523 20. Eliaz, D. *et al.* Exosome secretion affects social motility in *Trypanosoma brucei*. *PLoS*
524 *Pathog.* **13**, e1006245 (2017).
525 21. DeMarco, S. F., Saada, E. A., Lopez, M. A. & Hill, K. L. Identification of Positive Chemotaxis
526 in the Protozoan Pathogen *Trypanosoma brucei*. *mSphere* **5**, (2020).
527 22. Pozzo, L. Y. *et al.* Studying taxis in real time using optical tweezers: applications for
528 *Leishmania amazonensis* parasites. *Micron* **40**, 617–620 (2009).
529 23. Diaz, E. *et al.* Effect of aliphatic, monocarboxylic, dicarboxylic, heterocyclic and sulphur-
530 containing amino acids on *Leishmania spp.* chemotaxis. *Parasitology* **142**, 1621–1630
531 (2015).
532 24. Barros, V. C., Oliveira, J. S., Melo, M. N. & Gontijo, N. F. *Leishmania amazonensis*:
533 chemotaxic and osmotaxic responses in promastigotes and their probable role in
534 development in the phlebotomine gut. *Exp. Parasitol.* **112**, 152–157 (2006).
535 25. Lopez, M. A., Saada, E. A. & Hill, K. L. Insect stage-specific adenylate cyclases regulate
536 social motility in African trypanosomes. *Eukaryot. Cell* **14**, 104–112 (2015).
537 26. Imhof, S., Vu, X. L., Bütikofer, P. & Roditi, I. A Glycosylation Mutant of *Trypanosoma*
538 *brucei* Links Social Motility Defects In Vitro to Impaired Colonization of Tsetse Flies In
539 Vivo. *Eukaryot. Cell* **14**, 588–592 (2015).
540 27. Jelk, J. *et al.* Glycoprotein biosynthesis in a eukaryote lacking the membrane protein Rft1.
541 *J. Biol. Chem.* **288**, 20616–20623 (2013).

542 28. Shaw, S. *et al.* Flagellar cAMP signaling controls trypanosome progression through host
543 tissues. *Nat. Commun.* **10**, (2019).
544 29. Liniger, M. *et al.* Cleavage of trypanosome surface glycoproteins by alkaline trypsin-like
545 enzyme(s) in the midgut of *Glossina morsitans*. *Int. J. Parasitol.* **33**, 1319–1328 (2003).
546 30. Bringaud, F., Ebikeme, C. & Boshart, M. Acetate and succinate production in amoebae,
547 helminths, diplomonads, trichomonads and trypanosomatids: common and diverse
548 metabolic strategies used by parasitic lower eukaryotes. *Parasitology* **137**, 1315–1331
549 (2010).
550 31. Besteiro, S. *et al.* Succinate secreted by *Trypanosoma brucei* is produced by a novel and
551 unique glycosomal enzyme, NADH-dependent fumarate reductase. *J. Biol. Chem.* **277**,
552 38001–38012 (2002).
553 32. Lee, M. G., Bihain, B. E., Russell, D. G., Deckelbaum, R. J. & Van der Ploeg, L. H.
554 Characterization of a cDNA encoding a cysteine-rich cell surface protein located in the
555 flagellar pocket of the protozoan *Trypanosoma brucei*. *Mol. Cell. Biol.* **10**, 4506–4517
556 (1990).
557 33. Affolter, M., Hemphill, A., Roditi, I., Müller, N. & Seebeck, T. The repetitive microtubule-
558 associated proteins MARP-1 and MARP-2 of *Trypanosoma brucei*. *J. Struct. Biol.* **112**,
559 241–251 (1994).
560 34. Ebikeme, C. E. *et al.* N-acetyl D-glucosamine stimulates growth in procyclic forms of
561 *Trypanosoma brucei* by inducing a metabolic shift. *Parasitology* **135**, 585–594 (2008).
562 35. Ruepp, S. *et al.* Survival of *Trypanosoma brucei* in the tsetse fly is enhanced by the
563 expression of specific forms of procyclin. *J. Cell Biol.* **137**, 1369–1379 (1997).
564 36. Zheng, B., Yao, H. & Lee, G. S. Inactivation of the gene encoding the flagellar pocket
565 protein, CRAM, in African trypanosomes. *Mol. Biochem. Parasitol.* **100**, 235–242 (1999).
566 37. Gould, M. K. *et al.* Cyclic AMP effectors in African trypanosomes revealed by genome-
567 scale RNA interference library screening for resistance to the phosphodiesterase
568 inhibitor CpdA. *Antimicrob. Agents Chemother.* **57**, 4882–4893 (2013).
569 38. GEIGY, R., HUBER, M., WEINMAN, D. & WYATT, G. R. Demonstration of trehalose in the
570 vector of African trypanosomiasis: the tsetse fly. *Acta Trop.* **16**, 255–262 (1959).

571 39. Saada, E. A. *et al.* Insect stage-specific receptor adenylate cyclases are localized to
572 distinct subdomains of the Trypanosoma brucei Flagellar membrane. *Eukaryot. Cell* **13**,
573 1064–1076 (2014).
574 40. Wright, M. H., Paape, D., Price, H. P., Smith, D. F. & Tate, E. W. Global Profiling and
575 Inhibition of Protein Lipidation in Vector and Host Stages of the Sleeping Sickness
576 Parasite *Trypanosoma brucei*. *ACS Infect. Dis.* **2**, 427–441 (2016).
577 41. Kwon, H., Choi, M., Ahn, Y. & Pak, Y. N-myristoylation regulates insulin-induced
578 phosphorylation and ubiquitination of Caveolin-2 for insulin signaling. *Biochem. Biophys.*
579 *Res. Commun.* (2020) doi:10.1016/j.bbrc.2020.08.072.
580 42. Caljon, G. *et al.* The Dermis as a Delivery Site of *Trypanosoma brucei* for Tsetse Flies. *PLoS*
581 *Pathog.* **12**, e1005744 (2016).
582 43. Capewell, P. *et al.* The skin is a significant but overlooked anatomical reservoir for vector-
583 borne African trypanosomes. *Elife* **5**, (2016).
584 44. Trindade, S. *et al. Trypanosoma brucei* Parasites Occupy and Functionally Adapt to the
585 Adipose Tissue in Mice. *Cell Host Microbe* **19**, 837–848 (2016).
586 45. Cremer, J. *et al.* Chemotaxis as a navigation strategy to boost range expansion. *Nature*
587 **575**, 658–663 (2019).
588 46. Le Ray, D., Barry, J. D., Easton, C. & Vickerman, K. First tsetse fly transmission of the
589 'AnTat' serodeme of *Trypanosoma brucei*. *Ann. Soc. Belg. Med. Trop. (1920).* **57**, 369–381
590 (1977).
591 47. Overath, P., Czichos, J. & Haas, C. The effect of citrate/cis-aconitate on oxidative
592 metabolism during transformation of *Trypanosoma brucei*. *Eur. J. Biochem.* **160**, 175–182
593 (1986).
594 48. Brun, R. & Schönenberger. Cultivation and in vitro cloning or procyclic culture forms of
595 *Trypanosoma brucei* in a semi-defined medium. Short communication. *Acta Trop.* **36**,
596 289–292 (1979).
597 49. Lamour, N. *et al.* Proline metabolism in procyclic *Trypanosoma brucei* is down-regulated
598 in the presence of glucose. *J. Biol. Chem.* **280**, 11902–11910 (2005).
599 50. Roditi, I., Carrington, M. & Turner, M. Expression of a polypeptide containing a dipeptide

600 repeat is confined to the insect stage of *Trypanosoma brucei*. *Nature* **325**, 272–274
601 (1987).
602 51. Roditi, I. *et al.* Procyclin gene expression and loss of the variant surface glycoprotein
603 during differentiation of *Trypanosoma brucei*. *J. Cell Biol.* **108**, 737–746 (1989).
604 52. Knüsel, S. & Roditi, I. Insights into the regulation of GPEET procyclin during differentiation
605 from early to late procyclic forms of *Trypanosoma brucei*. *Mol. Biochem. Parasitol.* **191**,
606 66–74 (2013).
607 53. Allemann, N. & Schneider, A. ATP production in isolated mitochondria of procyclic
608 *Trypanosoma brucei*. *Mol. Biochem. Parasitol.* **111**, 87–94 (2000).
609 54. Gadelha, C., Wickstead, B., de Souza, W., Gull, K. & Cunha-e-Silva, N. Cryptic paraflagellar
610 rod in endosymbiont-containing kinetoplastid protozoa. *Eukaryot. Cell* **4**, 516–525 (2005).
611 55. Wheeler, R. J. Use of chiral cell shape to ensure highly directional swimming in
612 trypanosomes. *PLoS Comput. Biol.* **13**, e1005353 (2017).
613 56. Schindelin, J. *et al.* Fiji: An open-source platform for biological-image analysis. *Nat.*
614 *Methods* **9**, 676–682 (2012).
615 57. Florini, F., Naguleswaran, A., Gharib, W. H., Bringaud, F. & Roditi, I. Unexpected diversity
616 in eukaryotic transcription revealed by the retrotransposon hotspot family of
617 *Trypanosoma brucei*. *Nucleic Acids Res.* **47**, 1725–1739 (2019).
618 58. Al Kaabi, A., Traupe, T., Stutz, M., Buchs, N. & Heller, M. Cause or effect of arteriogenesis:
619 compositional alterations of microparticles from CAD patients undergoing external
620 counterpulsation therapy. *PLoS One* **7**, e46822 (2012).
621 59. Beneke, T. *et al.* A CRISPR Cas9 high-throughput genome editing toolkit for
622 kinetoplastids. *R. Soc. open Sci.* **4**, 170095 (2017).
623 60. Burkard, G., Fragoso, C. M. & Roditi, I. Highly efficient stable transformation of
624 bloodstream forms of *Trypanosoma brucei*. *Mol. Biochem. Parasitol.* **153**, 220–223
625 (2007).
626 61. Schumann Burkard, G., Jutzi, P. & Roditi, I. Genome-wide RNAi screens in bloodstream
627 form trypanosomes identify drug transporters. *Mol. Biochem. Parasitol.* **175**, 91–94
628 (2011).

Acknowledgements

Ruth Etzensperger, Berta Pozzi, Stephanie DeMarco and Boris Striepen are thanked for stimulating discussions and constructive comments on the manuscript. This research was supported by the Swiss National Science Foundation (Grant numbers 310030_184669 and 31003A_166427) and the Canton of Bern.

Author contributions

S.S., S.K., A.N., D.A. and I.R. conceived, designed and conducted experiments. All authors analysed the data. S.S. and I.R. wrote the paper.

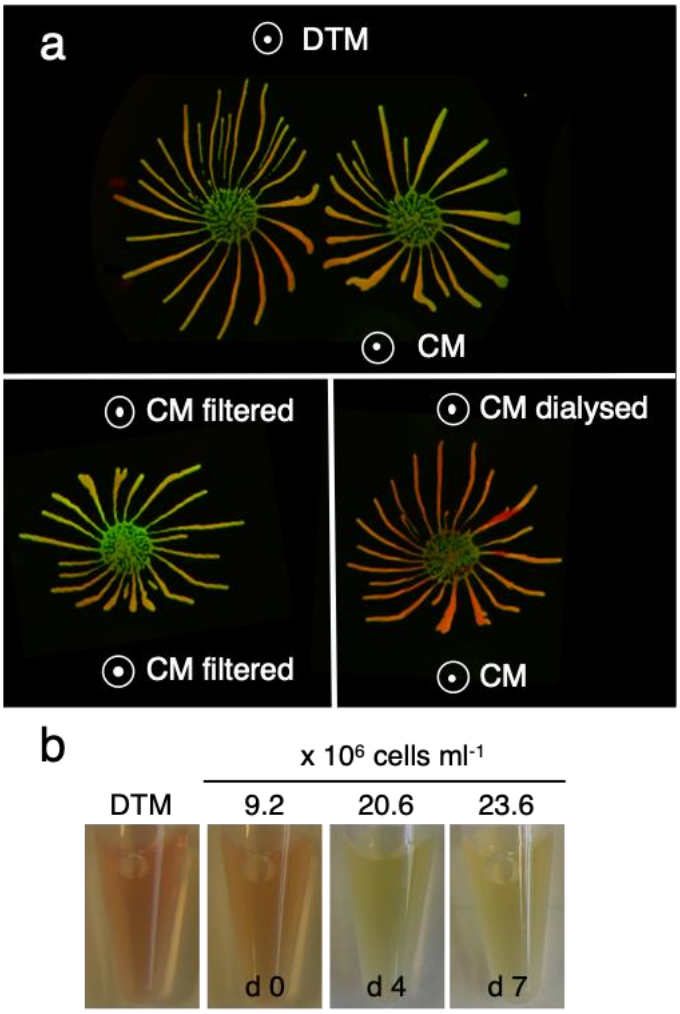

Fig. 1 Response of migrating cells to fresh medium (DTM) and conditioned medium (CM) after different treatments. **a** Upper panel: communities exposed to DTM and CM; lower left panel: communities exposed to filtered CM on both sides; lower right panel: communities exposed to dialysed CM (12 kDa cut-off) or undialysed CM. White circles with dots indicate where solutions were pipetted onto the plates. Community lifts stained for EP (green) and GPEET (red) are shown. **b** Continuous growth in liquid culture acidifies medium. Representative pictures of culture supernatants from early procyclic forms (EATRO1125) grown in DTM for 7 days without dilution. Left, DTM only. Samples were taken on days 0, 4 and 7. The colour change from red to yellow indicates that the culture becomes more acidic with time. Cell titres are indicated.

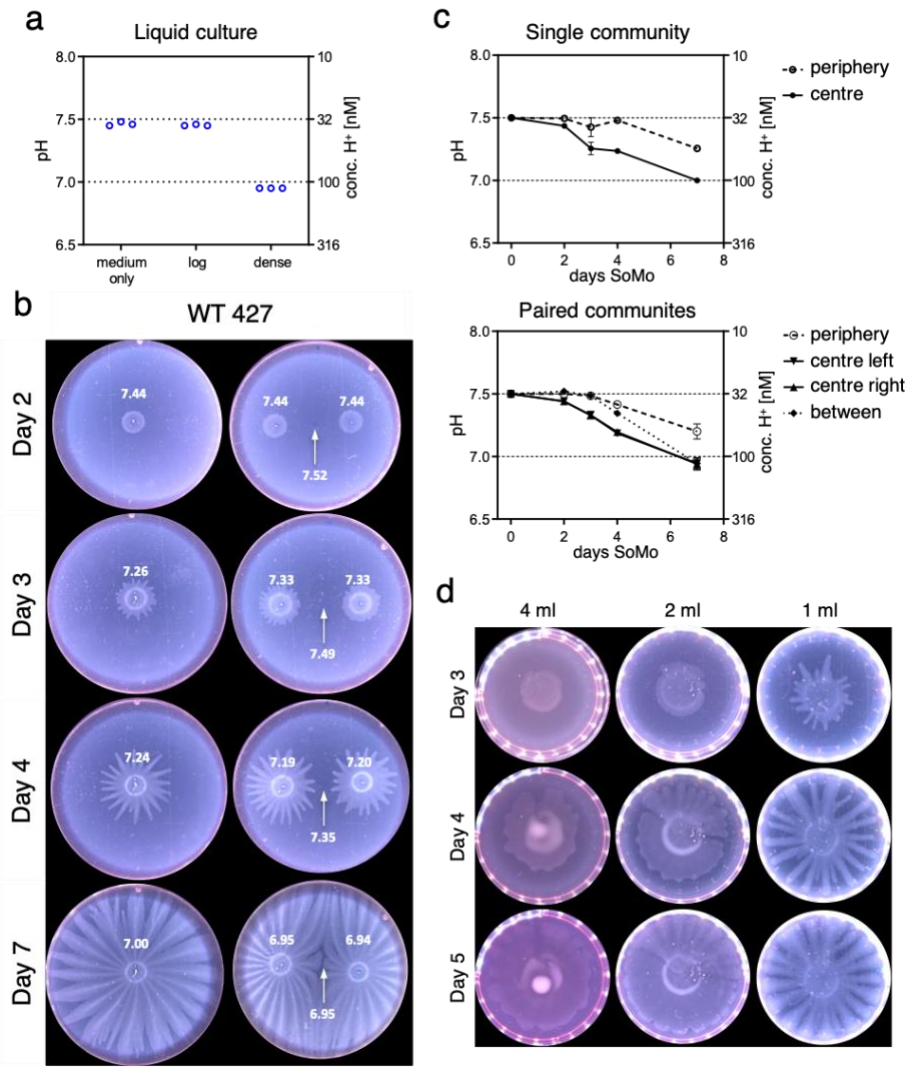

Fig. 2 Trypanosomes acidify their environment in liquid culture and on semi-solid agarose plates**.** Early procyclic forms (Lister 427 Bern) grown in SDM79 were analysed. **a** pH (left y axis) of medium only, a log-phase culture (log, 3.9 x 10^6 cells ml^{-1}) and a dense culture (dense, 5.6 x 10^7 cells ml^{-1}). Three technical replicates are shown. The H^+ concentration is indicated on the right y axis. Medium only was incubated for the same length of time as the cultures. **b** and **c** pH measurements on SoMo plates. **b** Trypanosomes (2 x 10^5 cells) were either spotted onto the centre of a plate as a single inoculum (left row) or in pairs (right row). White numbers indicate pH measurements on days 0, 2, 3, 4 and 7 in the centre of a community, at the periphery and in the space between two communities (indicated with a white arrow). **c** Graphs for pH measurement shown in **b**. Each data point represents the mean pH measured from replicate plates, error bars depict the range (n=2). Top: plates with single communities. pH at the plate periphery (○ dashed line) or in the centre of the community (● solid line). Bottom: paired communities. pH at the plate periphery (○ dashed line), in the centres of the two communities (▼ or ▲ solid line), or between them (◆ dotted line). Y axes are the same as in **a.**

d The time-point of migration depends on the volume of the substrate. Equal numbers of early procyclic forms were inoculated onto wells that contained different volumes of medium with agarose. Plates were photographed on days 3, 4 and 5 post inoculation.

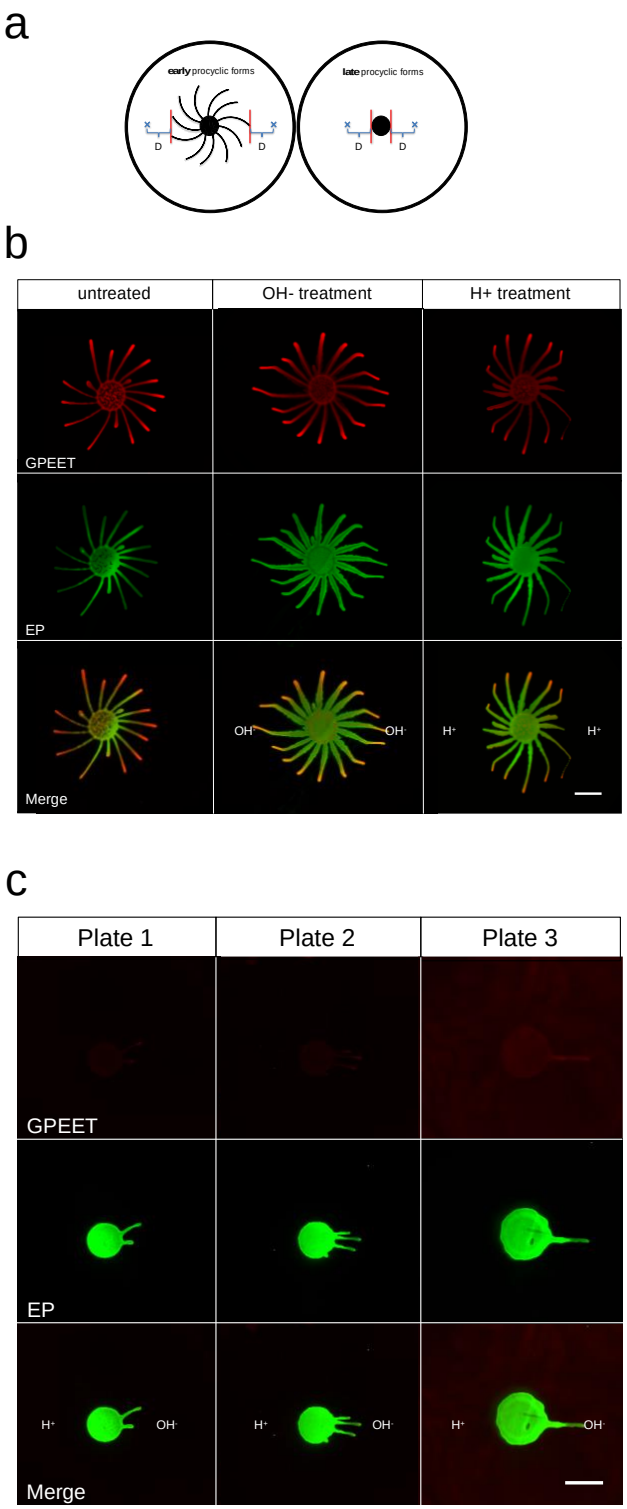

Fig. 3 Response of early and late procyclic forms to acidic or basic solutions. **a** Schematic representation of the pH taxis assay. "x" represents the site where a solution was spotted. "D" is the distance between the closest projection and the spot. In these experiments D= 1.3 cm. **b** Early procyclic forms (EATRO1125) on DTM plates were exposed to NaOH (OH- treatment) or HCl (H+ treatment) on both sides of the population. **c** Late procyclic forms were exposed to NaOH on the right side and HCl on the left side of the community. Scale bar: 1 cm. For **b** and **c** community lifts stained for EP (green) and GPEET (red) are shown.

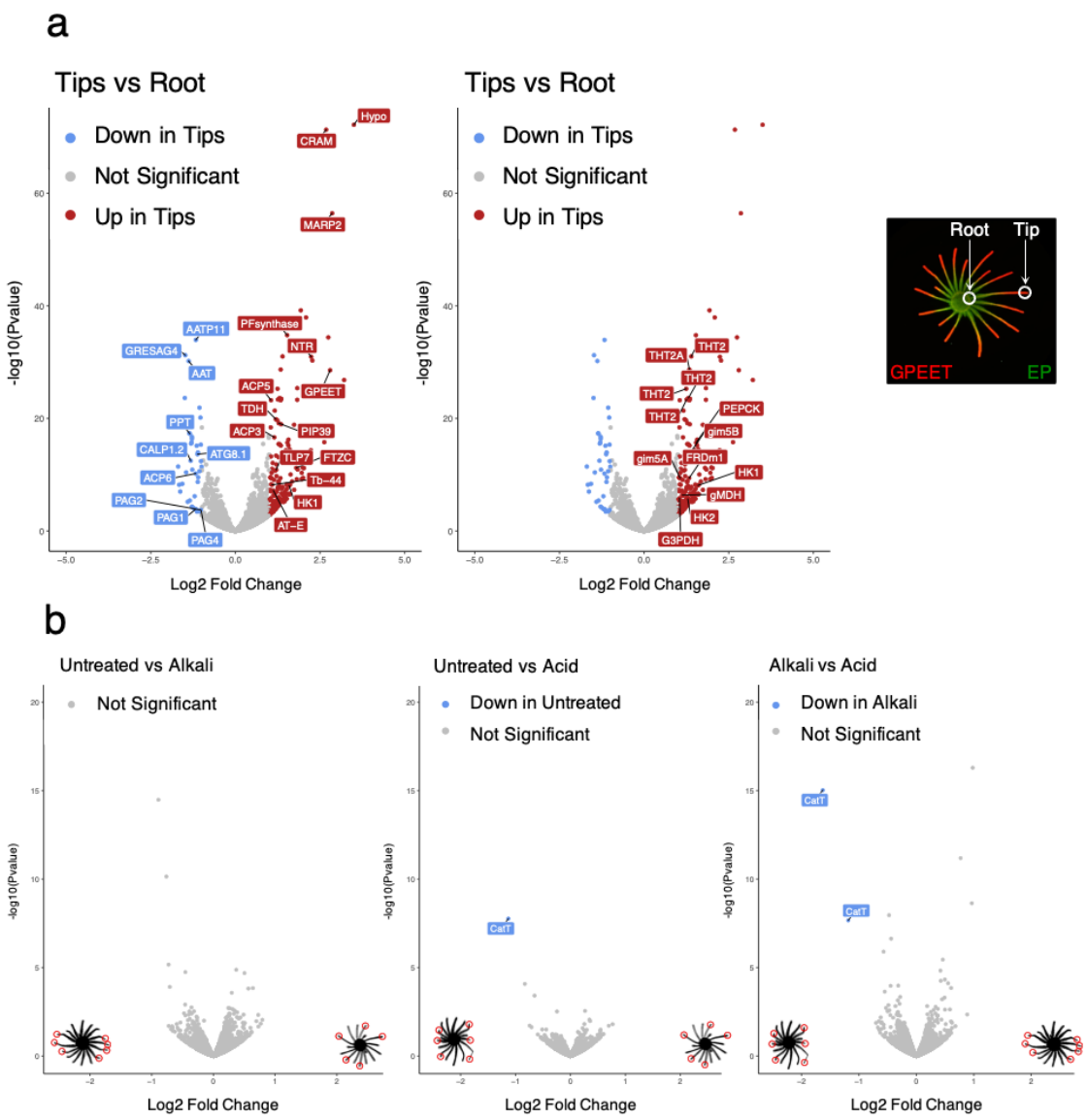

Fig. 4 Volcano plots comparing transcriptomes of cells from different regions of a community or following exposure to acid or alkali. DTM plates were inoculated with cells from liquid cultures of early procyclic forms (EATRO1125) in DTM medium. **a** Comparison of the roots and tips of projections. For clarity the same volcano plot is displayed twice with different transcripts annotated. Left: early procyclic form markers, such as GPEET, calflagin, hexokinase 1 and prostaglandin F synthetase are upregulated in tips. Adenylate cyclases such as ACP3, ACP5 and ACP6 are differentially expressed between tip and root. Right: glycolytic enzymes and genes involved in glucose metabolism are upregulated in tips. Far-right panel: community lift of a representative SoMo plate 7 days after inoculation stained for EP (green) and GPEET (red). Tips were isolated when projections were ≥ 2.5 cm in length. RNA-seq was performed in duplicate. **b** Pairwise comparisons of untreated communities and communities exposed to acid or alkali. Tips were isolated from projections showing a clear response to the treatment (indicated with red circles). RNA-seq was performed in triplicate. The illlustrations in the left and right bottom corners of the volcano plots show SoMo communities (in black) and the samples that were collected (red circles).

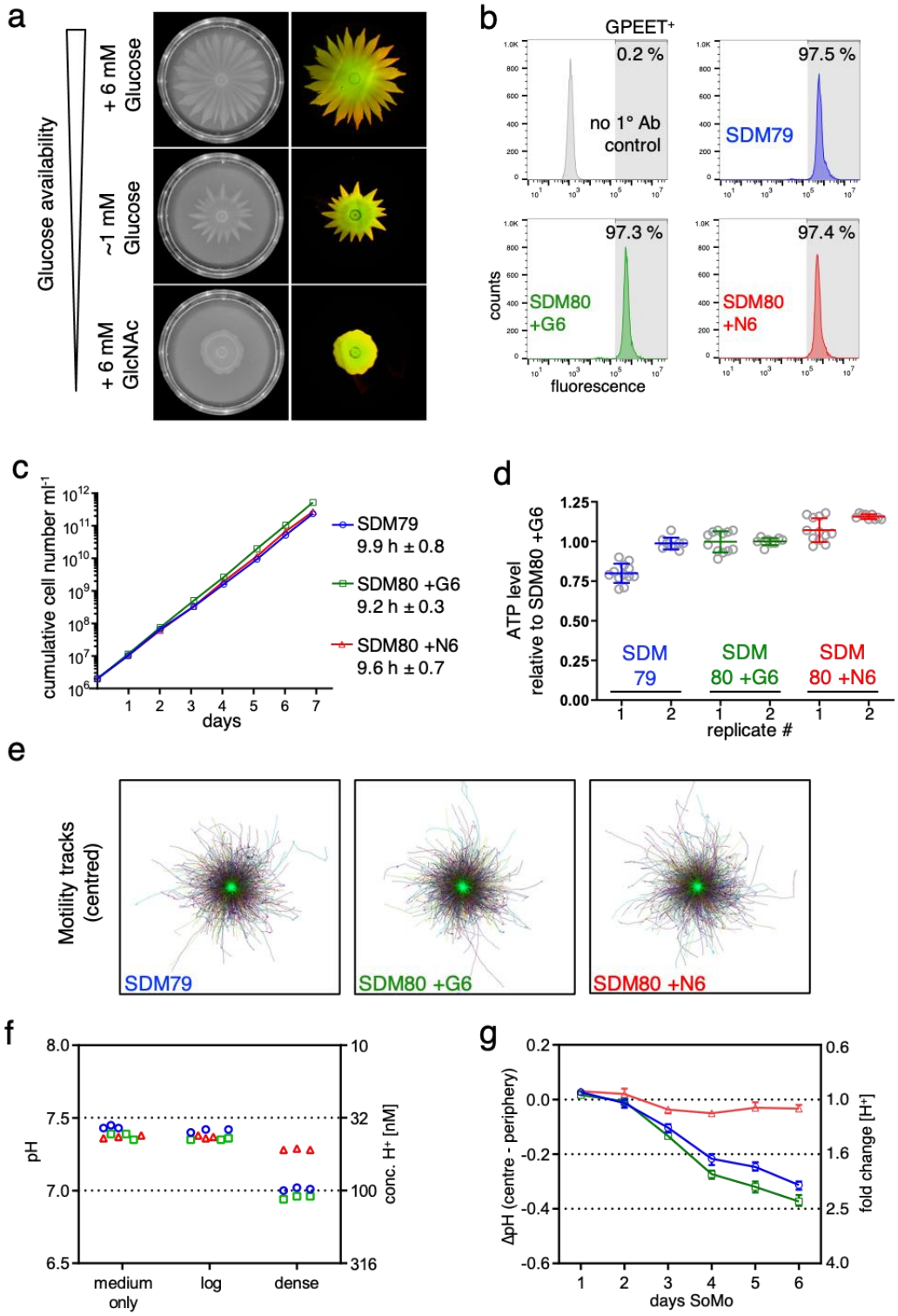

Fig. 5 Glucose availability impacts SoMo by acidification of the culture medium. Procyclic forms (Lister 427 Bern) grown in SDM79 or SDM80 plus supplements were analysed: SDM79 (blue / ○), SDM80+G6 (+ 6 mM glucose, green / □), SDM80+N6 (+ 6 mM GlcNAc, red / △). If not specified, cells were adapted from SDM79 to the medium indicated for one to three weeks. **a** Social motility on semi-solid plates was

685 assessed in SDM80 with varying glucose availability. Left: SoMo plates on day 6 after inoculation, prior to
686 performing community lifts. Cells were adapted from SDM80+G6 to the corresponding liquid medium for
687 5 days before inoculation. Right: merge of the corresponding community lifts probed for GPEET (red) and
688 EP (green). **b** Flow cytometric analysis. The percentage of GPEET-positive cells (shaded area) is indicated.
689 Cells grown in SDM79 were used as a control (2° antibody only, grey). **c** Cumulative growth in different
690 media. Growth was monitored after transferring cells from SDM79 to the corresponding medium 3 days
691 earlier. Numbers indicate population doubling time averaged over 7 days (mean ± SD). **d** Steady-state ATP
692 levels in different media. Cell lysates were harvested in two independent experiments (replicate 1 or 2,
693 respectively). Cell densities at harvest were between 6.2 - 8.0 or 7.3 - 8.9 x 10^6 cells ml^{-1}, respectively.
694 Appropriate dilutions of cell lysates were assayed; the graph depicts means and error bars (SD) of technical
695 replicates shown as circles (n=12 or 9, respectively). Data are shown relative to SDM80+G6. **e** Directional
696 motility in different media. Cell densities at harvest were between 5.9 - 6.5 x 10^6 cells ml^{-1}. Centred motility
697 tracks of individual cells are shown at identical scale. > 6000 tracks in each medium were pooled from
698 nine movies acquired from three technical replicates.
699 **f** pH measurement of liquid cultures. Culture medium (medium only) and supernatants from log-phase
700 (log) or dense culture (dense). Cell titres per ml in SDM79, SDM80+G6 or SDM80+N6, respectively: 3.2 x
701 10^6, 3.8 x 10^6 or 3.3 x 10^6 (log) and 5.1x 10^7, 4 x 10^7or 3.6 x 10^7 (dense). Three technical replicates are
702 shown for each condition. The corresponding H^+ concentration is indicated on right y axis. **g** pH
703 measurements on SoMo plates inoculated with cells pre-adapted to the corresponding liquid medium.
704 ΔpH (centre − periphery) refers to pH in centre of the community minus the pH at the plate periphery.
705 Each data point represents the mean ΔpH from replicate plates, error bars depict the range (n=3). The
706 fold change in H^+ concentration is indicated on the right y axis.

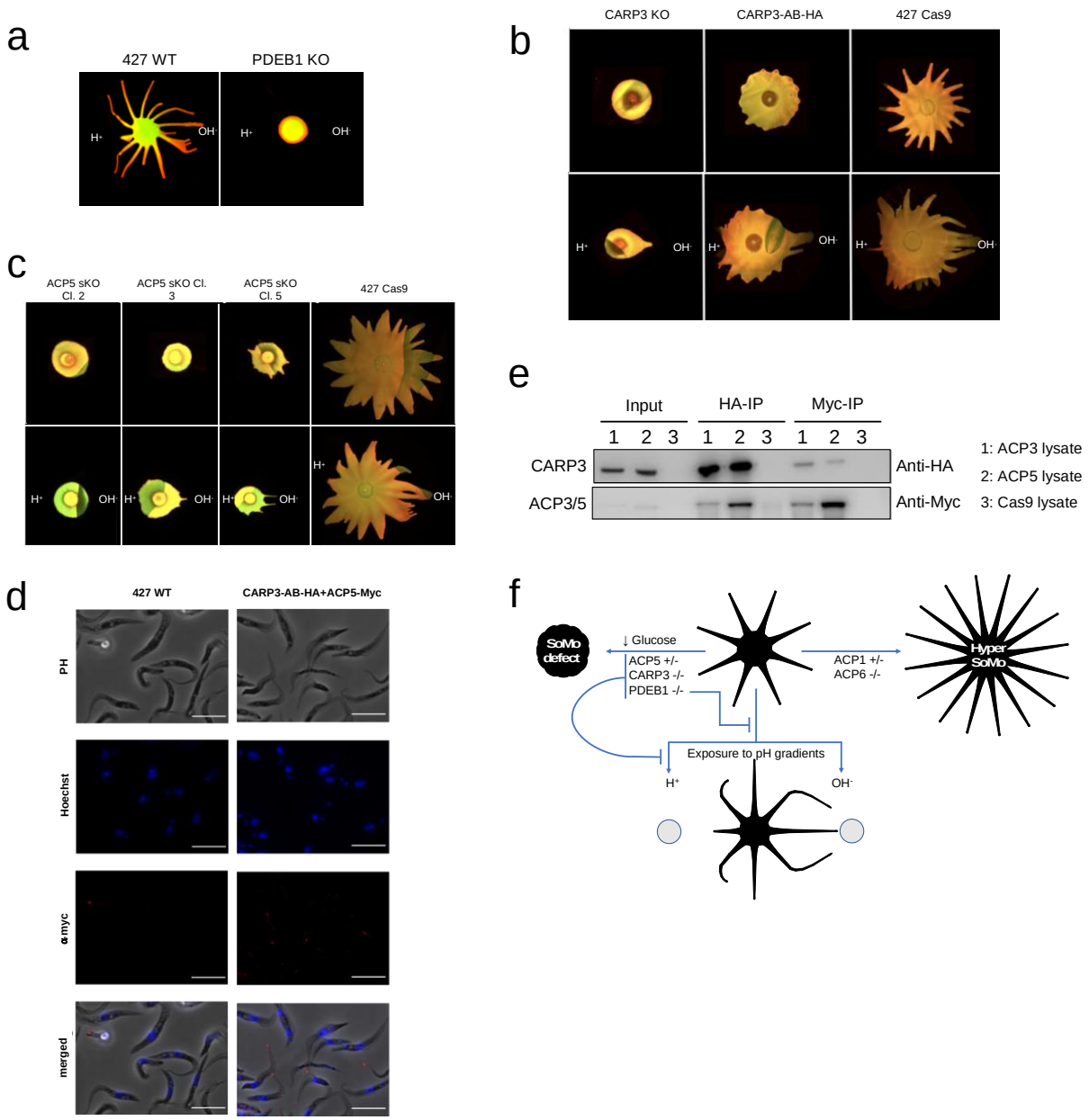

Fig. 6 pH responses by SoMo-defective mutants. **a-c** Community lifts labelled with anti-GPEET (red) and anti-EP (green). The images in **a**, **b**, and **c** show merged EP and GPEET signals. **a** Lister 427 wt and PDEB1 knockout (KO). **b** 427 Cas9 parental line, CARP3-KO and CARP3-HA addback. Upper panel: untreated. Lower panel: exposed to acid and alkali. **c** 427 Cas9 parental line and 3 independent ACP5 single allele knockouts; panels as in **b**.

d Myc-tagged ACP5 is localised to the flagellar tip in a cell line co-expressing CARP3-HA. Immunofluorescence was performed with an anti-myc antibody (red). DNA was stained with Hoechst dye. Scale bar = 10 µm. **e** Western blot analysis of immunoprecipitations with anti-HA and anti-myc antibodies. Myc-tagged ACP3 and ACP5 were expressed independently in the CARP3-HA background. The parental line 427 Cas9 was used as a control. Input samples have 40 times fewer cell equivalents than the

717 immunoprecipitated samples. IP: immunoprecipitation with anti-HA or anti-myc antibodies. **f** Summary of
718 mutants, SoMo phenotypes and responses to pH. -/-: double knockouts; +/-: single knockouts.

719 **Supplementary data**

720 All supplementary figures, tables and movies are available via the following link:
721 https://www.dropbox.com/sh/r7od7e0s5j04g3m/AAD3wUFIbHjKGeFavE27ndAxa?dl=0
722
723 **Supplementary Fig. 1** Different chemicals were tested for their impact on migrating cells on semi-
724 solid surfaces. Procyclic forms of EATRO1125 were incubated on DTM plates. **a** All chemicals
725 were dissolved or diluted in water to give 1 M solutions. Chemicals highlighted in red could not
726 be dissolved completely, but were used anyway. **b** Effect on migrating cells and pH of 1M
727 solutions. **c** SoMo assays. Chemicals were spotted on day 4 after inoculation and photographs
728 were taken 16-20 h later. Photographs were processed to improve contrast and converted to
729 black and white.
730
731 **Supplementary Fig. 2** Independent CRAM knockout clones exposed to acid and alkali. **a** Upper
732 panel: community lifts of CRAM knockout clones and their 427 Cas9 parental cell line. Lower
733 panel: community lifts of knockouts and the parental line exposed to acid (H^+) and alkali (OH^-).
734 The images show merged EP and GPEET signals. **b** Growth comparison of three individual CRAM
735 knockouts and parental 427 Cas9.
736
737 **Supplementary Fig. 3** Characterisation of CARP3 and CARP4 knockouts. **a** Genotyping of CARP3
738 and CARP4 knockouts by PCR. Genomic DNA was isolated from individual clones and amplified
739 with the primers listed in Supplementary Table 3. **b** Growth comparison of CARP3 and CARP4
740 knockouts and parental 427 Cas9. **c** Motility assay of CARP3 knockouts. Centred motility tracks of
741 individual cells are shown at identical scale. > 8000 tracks for each cell line (427 Cas9, CARP3 KO
742 Cl.1, CARP3 KO Cl.2 and Trypanin KO, respectively) were pooled from nine movies acquired from
743 three technical replicates. The trypanin knockout was used as a motility-
744 deficient control[28]. **d** Velocity and speed of each cell line. The colour code corresponds to the cell
745 lines in d. Data points are displayed as box plot with whiskers representing 2.5 - 97.5 percentile,
746 filled circles represent points outside that range. InterQuartileRange IQR (25 - 75 percentile), with
747 Median (50 percentile). **e** Percentage of GPEET-positive cells (shaded area) is indicated. Cells
748 without prior incubation with anti-GPEET antiserum were used as a negative control (2° antibody
749 only, grey). **f** Localisation of CARP3-HA (green) by immunofluorescence. DNA was stained with
750 Hoechst dye. Scale bar = 10 µm.
751
752 **Supplementary Fig. 4** Characterisation of ACP knockouts. **a** Genotyping of ACP knockouts by PCR.
753 Genomic DNA was isolated and PCRs were performed with the primers listed in Supplementary

754 Table 3. **b** SoMo and pH taxis assays. Plates were inoculated with the cell lines indicated and 4
755 days later HCl and NaOH were applied to the plates (indicated by dots). Pictures were taken 16-
756 20 h after spotting of chemicals. **c** Growth of ACP5 single knockout clones compared to the
757 parental 427 Cas9 cell line. **d** Motility assays of ACP5 single knockouts. Centred motility tracks of
758 individual cells are shown at identical scale. > 7000 tracks for each clone were pooled from nine
759 movies acquired from three technical replicates. The parental line 427 Cas9 and Trypanin KO
760 were used as controls. **e** Velocity and speed of individual cell lines. The colour code corresponds
761 to the cell lines in d. Data points are displayed as box plot with whiskers representing 2.5 - 97.5
762 percentile, filled circles represent points outside that range. InterQuartileRange IQR (25 - 75
763 percentile), with Median (50 percentile). **f** Flow cytometric analysis of percentages of GPEET-
764 positive cells.
765
766 **Supplementary Table 1** RNAseq data. **a** Comparison of the roots and tips of projections.
767 Transcripts from the tips either upregulated >1 Log2FC or downregulated <1 Log2FC in
768 comparison to the root. FC: fold change. **b** Pairwise comparisons of untreated communities and
769 communities exposed to acid or alkali. Transcripts from tips that were either upregulated >1
770 Log2FC or downregulated <1 Log2FC. FC: fold change.
771 Raw read files are deposited at the European Nucleotide Archives (ENA)
772 http://www.ebi.ac.uk/ena as study PRJEB41935.
773
774 **Supplementary Table 2** ACP3 and ACP5 are immunoprecipitated with CARP3-HA.
775
776 **Supplementary Table 3** List of primers used for knockouts and genotyping.
777
778 **Supplementary Video 1** Early procyclic form parasites exhibit social motility.
779
780 **Supplementary Video 2** Response of early procyclic forms to hydrochloric acid (HCl). Black arrows
781 indicate where solutions were spotted. The video is shown as a rewind loop.
782
783 **Supplementary Video 3** Response of early procyclic forms to sodium hydroxide (NaOH). Black
784 arrows indicate where solutions were spotted. The video is shown as a rewind loop.
785
786 **Supplementary Video 4** Response of late procyclic forms to sodium hydroxide (NaOH). Black
787 arrows indicate where solutions were spotted. The video is shown as a rewind loop.